JACC: CARDIOVASCULAR INTERVENTIONS
VOL. 7, NO. 10, 2014

ISSN 1936-8798/$36.00
PUBLISHED BY ELSEVIER INC.
http://dx.doi.org/10.1016/j.jcin.2014.04.024

VIEWPOINT

Methodological Standardization for the Pre-Clinical Evaluation of Renal Sympathetic Denervation

Kenichi Sakakura, MD,* Elena Ladich, MD,* Elazer R. Edelman, MD,† Peter Markham, MS,†
James R.L. Stanley, DVM,† John Keating, DVM,† Frank D. Kolodgie, PhD,* Renu Virmani, MD,* Michael Joner, MD*

ABSTRACT

Transcatheter ablation of renal autonomic nerves is a viable option for the treatment of resistant arterial hypertension; however, structured pre-clinical evaluation with standardization of analytical procedures remains a clear gap in this field. Here we discuss the topics relevant to the pre-clinical model for the evaluation of renal denervation (RDN) devices and report methodologies and criteria toward standardization of the safety and efficacy assessment, including histopathological evaluations of the renal artery, periarterial nerves, and associated periadventitial tissues. The pre-clinical swine renal artery model can be used effectively to assess both the safety and efficacy of RDN technologies. Assessment of the efficacy of RDN modalities primarily focuses on the determination of the depth of penetration of treatment-related injury (e.g., necrosis) of the periarterial tissues and its relationship (i.e., location and distance) and the effect on the associated renal nerves and the correlation thereof with proxy biomarkers including renal norepinephrine concentrations and nerve-specific immunohistochemical stains (e.g., tyrosine hydroxylase). The safety evaluation of RDN technologies involves assessing for adverse effects on tissues local to the site of treatment (i.e., on the arterial wall) as well as tissues at a distance (e.g., soft tissue, veins, arterial branches, skeletal muscle, adrenal gland, ureters). Increasing experience will help to create a standardized means of examining all arterial beds subject to ablative energy and in doing so enable us to proceed to optimize the development and assessment of these emerging technologies. (J Am Coll Cardiol Intv 2014;7:1184–93) © 2014 by the American College of Cardiology Foundation.

The renal autonomic nervous system plays a major role in the development of arterial hypertension (1). Despite the adoption of contemporary pharmacological treatment, a substantial proportion of patients remain at high risk of subsequent cardiovascular and cerebrovascular events due to unexplained resistance to drug treatment (2). Renal sympathetic denervation has recently been

From the *CVPath Institute, Inc., Gaithersburg, Maryland; and †CBSET, Inc., Lexington, Massachusetts. This paper would not have been possible without the support of the following companies: Biosense Webster, Medtronic, Kona Medical, and ReCor Medical. None of the mentioned companies provided financial support for the preparation of the current manuscript. However, this consensus document is based on studies that were conduced in cooperation with the above mentioned companies. CVPath Institute, Inc. provided full support for the work of Drs. Sakakura, Ladich, Kolodgie, Virmani, and Joner. Dr. Edelman was supported by grants from the National Institutes of Health including R01 GM49039. P. Markham, Dr. Keating, and Dr. Stanley were supported by CBSET, Inc., Lexington, Massachusetts. Dr. Sakakura is supported by a research fellowship from the Banyu Life Science Foundation International. Dr. Sakakura has received speaking honoraria from Abbott Vascular, Boston Scientific, and Medtronic CardioVascular. Dr. Virmani receives research support from 480 Biomedical, Abbott Vascular, Atrium, Biosensors International, Biotronik, Boston Scientific, CeloNova, Cordis J&J, GlaxoSmithKline, Kona, Medtronic, Microport Medical, OrbusNeich Medical, ReCor Medical, SINO Medical Technology, Terumo Corporation, and W.L. Gore; Dr. Virmani is a speaker for Merck; and receives honoraria from 480 Biomedical, Abbott Vascular, Biosense Webster, Biosensors International, Boston Scientific, Claret Medical, CeloNova, Cordis J&J, Lutonix, Medtronic, Terumo Corporation, and W.L. Gore; and is a consultant for 480 Biomedical, Abbott Vascular, Medtronic, and W.L. Gore. Dr. Joner is a consultant for Biotronik and Cardionovum; and has received speaker honoraria from Abbott Vascular, Biotronik, Cordis J&J, Medtronic, and St. Jude Medical. All other authors have reported that they have no relationships relevant to the contents of this paper to disclose.

Manuscript received February 4, 2014; revised manuscript received April 22, 2014, accepted April 23, 2014.

introduced as a promising option for the treatment of resistant hypertension. Indeed, catheter-based radiofrequency renal denervation (RDN) has demonstrated effectiveness in clinical studies (3). The increasing prevalence of patients with resistant hypertension on a global scale (2) and the appeal of definitive intervention without lifelong obligate adherence to repeated drug dosing has generated a fierce demand to refine current catheter-based RDN procedures and technologies. To this effect, a variety of technological innovations such as radiofrequency and ultrasound catheters, catheter-based microinfusion of neurotoxic drugs, and externally applied focused ultrasound have been developed, and pre-clinical studies for those devices are ongoing (4). The main objective of these technological endeavors pertains to the effective destruction of periarterial sympathetic nerves while preserving arterial morphology and renal function.

In this regard, histopathological assessment of the renal vasculature, along with biomarker analysis of hormones and neurotransmitters, surrounding sympathetic nerves and other regional soft-tissue structures is critically important. However, there remains a clear lack of standardization with respect to the histopathological assessment of these tissues after denervation procedures. Most recently, the failure of the first randomized, sham-controlled clinical trial (SYMPLICITY HTN-3 [Renal Denervation in Patients With Uncontrolled Hypertension]) to reach its primary efficacy endpoint at 6 months underscores the need to revisit existing pre-clinical animal models (5) because there is no marker of procedural efficacy (i.e., confirmation of effective and complete denervation) in humans. In this regard, we aim to establish standardized and reproducible methodology and criteria for histopathological evaluation after renal sympathetic denervation.

ANIMAL MODEL SYSTEMS

There are a number of means of applying energy to the arterial bed and a number of animal models in which such energies can be applied. The early literature in this field dates back to the groundbreaking work of Goldblatt et al. (6) who in the 1930s imposed unilateral or bilateral renal arterial constriction to provoke ischemia and the release of renin to induce hypertension. Their work in dogs defined renal vascular hypertension, helped to define the renin-angiotensin-aldosterone system, and was followed soon thereafter by a series of experiments demonstrating surgical sympathectomy as a possible therapeutic intervention. Other renal injury models emerged including complete ablation or excision of a kidney or infusion of nephrotoxins systemically or locally (7). Other species were considered including small rodents, especially the rat, and occasionally the rabbit (8). As percutaneous technologies have emerged, swine has become a preferred target. Although the bulk of studies are performed in intact animals, it will be increasingly the case that animals with modified renal vasculature and preceding hypertension will be considered. As these models emerge, careful comparison to control states must be attained. Such a definition needs to include not only architecture at a defined period of time but the temporal and spatial kinetics of the dynamics and recognition of systemic and circulating effects. These models therefore expand dramatically the tools available to examine ablative technologies but also simultaneously expand the challenges of careful and precise delineation of effects. Disease models necessarily disrupt the normal architecture, and our view of the normal state is inadequate. Each applied neurotoxic effect is accompanied by idiosyncratic changes, and these must be fully defined before we can proceed with understanding how therapeutic interventions play a role. It will now be especially important as well to track effects over time; we do not know, for example, whether there is recovery of neural ablation. Clinical studies seem to foretell sustained effects, but there is not a definitive time when recovery is observed or deemed beyond approach. As disease models are used, these time-dynamic effects will need to be pursued further.

ABBREVIATIONS AND ACRONYMS

CGRP = calcitonin gene-related peptide

H&E = hematoxylin and eosin

RDN = renal denervation

TH = tyrosine hydroxylase

TTC = 2,3,5-triphenyltetrazolium chloride

PORCINE RENOVASCULAR ANATOMY

Although animal models for the assessment of renal sympathetic denervation remain under development, the swine model is the most frequently used because of its similarity to the renovascular anatomy and size in humans (9). Nevertheless, descriptions of porcine perirenal nerve anatomy remain meager. We examined 11 normal renal arteries from 11 pigs to elucidate renovascular anatomy in this species. A total of 6 to 8 sections from each renal artery and surrounding tissues were sectioned at 4- to 5-mm intervals after marking with indelible ink of the ventral (orange), dorsal (black), superior (blue), and inferior (green) regions and subjected to routine tissue processing, paraffin embedding, sectioning at 4 to 5 μm, and staining with hematoxylin and eosin (H&E) and Movat pertachrome stains. Digital images were prepared from H&E-stained sections

at 1.25× magnification. Images were divided into 4 quadrants and analyzed using image analysis software (IP Lab for Mac OS X, Scanalytics, Rockville, Maryland). Length measurements from the luminal surface of the renal artery to the outer nerve contour were performed in each of the 4 quadrants (ventral, dorsal, superior, and inferior locations). Representative images of distance measurements are shown in Online Figure 1.

The mean length of renal arteries (from the aorta to renal artery bifurcation after removal and perfusion fixation by 10% formalin) was 2.1 ± 0.5 cm. A total of 484 nerves from 11 renal arteries were identified from 39 sections (mean number of nerves per section was 12.4 ± 5.7). The mean number of nerves in segments proximal (10.5 ± 6.2), middle (12.0 ± 4.4), and distal (14.0 ± 4.4) to the renal aortic ostium were not significantly different, although there was a trend toward greater nerves in the distal versus proximal ($p = 0.55$ for proximal vs. middle, $p = 0.06$ for proximal vs. distal, $p = 0.34$ for middle vs. distal). The mean number of nerves in the ventral location (4.7 ± 2.3) was significantly greater compared with the dorsal location (2.3 ± 1.1) ($p = 0.02$), whereas there was a similar number of nerves in the superior (3.0 ± 1.8) and inferior (2.1 ± 1.2) ($p = 0.19$) arterial location. The cumulative incidence of nerves at distance from lumen is shown in **Figure 1**. These data are somewhat at odds with those of Tellez et al. (10) who, using renal artery nerve distribution from 5 pigs, reported higher nerve density in the proximal segments compared with that in the middle or distal segments. Yet both studies confirmed nerve density in normal swine is less than in diseased humans (11), and, as such, if these spatial differences continue to be validated, they will not only influence the design of technology but necessitate careful maintenance of specimen alignment and location before effects can be adequately described or compared. Pre-clinical safety assessment including the study of porcine nerve anatomy is important for a standardized evaluation of innovative technology targeted at RDN therapy. However, the findings of pre-clinical studies should be interpreted with caution, as the influence of underlying atherosclerosis in human arteries as well as the depth of the nerve distribution may be different and cannot be assessed in healthy animal models. Moreover, as discussed previously, further examination of diseased animal model systems will likely soon follow.

NOREPINEPHRINE ANALYSIS

Researchers have determined that catecholamines such as norepinephrine are important biomarkers that aid in the evaluation of the efficacy of novel therapies in many disease states including neurological disorders, metabolic disease, pain, heart disease, and more specifically drug-resistant hypertension. Down-regulation of norepinephrine in renal

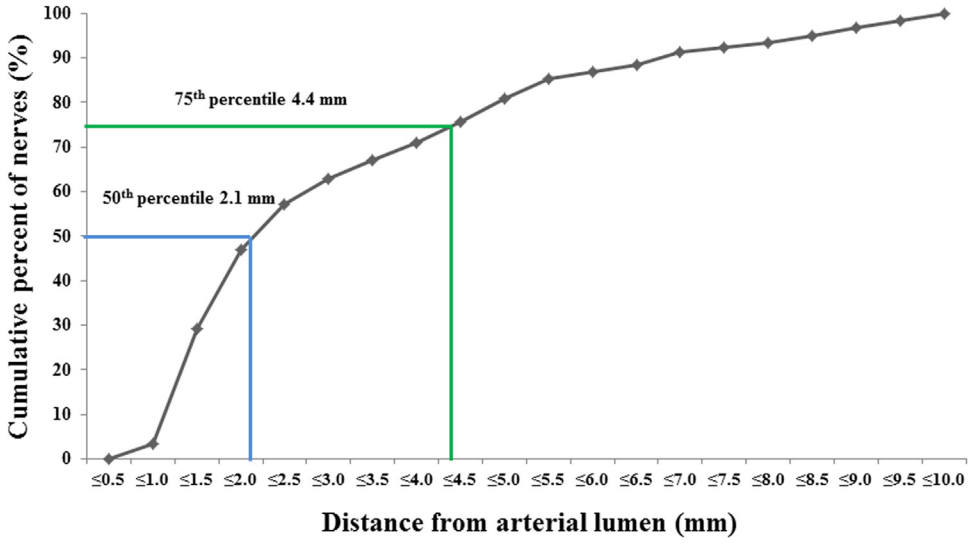

FIGURE 1 Cumulative Incidence of Normal Perirenal Nerve Distances From the Renal Arterial Lumen

The cumulative incidence of nerve distance from the lumen is calculated from 484 nerves. The 50th percentile of the distance from the arterial lumen to the nerve was 2.1 mm, whereas the 75th percentile was 4.4 mm.

tissue has been shown to be an indicator of the efficacy of RDN therapy in the treatment of drug-resistant hypertension (12,13). The analytical challenges present in the quantitative analysis of norepinephrine in renal tissue are significant. Norepinephrine is present at extremely low endogenous levels and is subject to extremely rapid metabolic and nonmetabolic oxidative degradation. Renal tissue collection techniques must be optimized to avoid autolysis, and tissues must be rapidly frozen before extraction. Tissue sampling techniques must ensure homogeneous sampling as norepinephrine is nonuniformly distributed in the kidney. Studies designed to correlate histopathological findings with norepinephrine levels must further combine rapid sampling and stabilization of kidney tissue to avoid norepinephrine degradation and perfusion fixation of the arterial and periarterial tissue to optimize nerve assessment.

Historical analytical methods of detection of norepinephrine have typically used high-pressure liquid chromatography coupled with electrochemical detection (14). High-pressure liquid chromatography coupled with electrochemical detection affords high sensitivity but lacks mass specificity and is therefore subject to potential interferences from a large number of endogenous and exogenous compounds.

The preferred method to quantify norepinephrine in swine renal tissue in the subendogenous range is high-throughput tandem mass spectrometry (15). Mass specificity provides the ability to differentiate norepinephrine from epinephrine and other endogenous catecholamines. Methods that use a stable isotope-labeled analyte (16), norepinephrine D_6, as a surrogate reference standard can leverage the fact that the deuterium-labeled norepinephrine and unlabeled norepinephrine behave uniformly during extraction, chromatography, and tandem mass spectroscopy ionization conditions. Extraction and homogenization of norepinephrine from pig kidney tissue must use a solution that helps to enhance the stability of norepinephrine. Through the use of the stable labeled compounds high-throughput tandem mass spectrometry can be used to determine norepinephrine at >2 orders of magnitude below endogenous levels. Tissue norepinephrine concentrations in the kidney of the treated arteries are then compared with the tissue norepinephrine concentration in the contralateral untreated kidney or to a pool of control animals (Online Figure 2), and norepinephrine data are presented as the percentage of norepinephrine reduction from control.

Methods of fixation and tissue dissection are described in the Online Appendix.

MACROSCOPIC 2,3,5-TRIPHENYLTETRAZOLIUM CHLORIDE STAINING

It is useful in the early phase of energy-based ablative device development to macroscopically examine the luminal surface of acutely treated renal arteries using 2,3,5-triphenyltetrazolium chloride (TTC) staining. TTC is not a true stain but a water-soluble salt that is enzymatically reduced by living cells to a formazan compound that imparts a visibly red coloration (17). TTC staining has been used for decades in research models for the detection and identification of tissue injury/necrosis (e.g., myocardial [18] or cerebral [19] infarction) as nonviable cells lack functional enzymatic processes and do not "stain" but remain pale, in stark contrast to the intensely red coloration of adjacent viable tissue. As such, the exposure of the lumen of acutely treated renal arteries to a TTC solution allows the precise delineation of the "footprint" of the energy modality and allows one to make macroscopic measurements and correlations with device and histological parameters.

HISTOPATHOLOGICAL AND IMMUNOHISTOCHEMICAL STAINS

Treatment-related soft-tissue damage can sometimes be visualized grossly during dissection; however, arterial, nerve, and soft-tissue damages are best visualized on H&E-stained sections. Additional stains of elastic fibers (e.g., elastica van Gieson, Movat pentachrome, or Mallory trichrome stains) are encouraged as these may provide helpful information with regard to changes in arterial morphology and tissue responses. Immunohistochemical staining for nerve fascicles should be considered in selected sections to evaluate for changes in neurotransmitters or axonal degeneration. Immunostains against S-100 protein (a marker for Schwann and sustentacular cells), neurofilament protein (a marker for neurons and ganglion cells), and glial fibrillary acidic protein (a marker for glial cells) are used for the recognition of nerve fascicles (20), whereas stains targeted at tyrosine hydroxylase (TH), which converts tyrosine to L-DOPA, are used for the presence or absence of norepinephrine synthesis (21). Although L-DOPA decarboxylase (which converts L-DOPA to dopamine) is another catecholamine-synthesizing enzyme, immunostaining against L-DOPA decarboxylase is rarely used in the area of RDN because L-DOPA decarboxylase-positive fibers are more sparsely distributed than TH-positive fibers in perivascular nerves in the kidney (22). The combination of at least 1 axonal

marker (S-100 protein, neurofilament protein, or glial fibrillary acidic protein) and a functional marker (TH) may provide meaningful insights into the functional relevance of ablative treatment against resistant hypertension.

Periarterial nerves around the kidney comprise efferent (sympathetic) nerve fibers and afferent (sensory) nerve fibers, and both types of nerves may affect renal sympathetic nerve activity (23). To identify renal afferent nerves, immunostains against calcitonin gene-related peptide (CGRP) and substance P, which serve as neurotransmitters in sensory nerves (24), have been reported in the literature. However, because immunostaining for CGRP using color-producing reagents has been reported to result in low intensity, the more reliably strong intensity of TH is most often adopted for staining of efferent sympathetic nerve fibers in the immunohistochemical assessment of successful ablation of periarterial sympathetic nerves (10). Most importantly, the intensity of color reaction has been shown to be correlated with presence of viable efferent sympathetic nerve fibers using TH staining (21), an association not found with other immunostain procedures such as CGRP and substance P.

EVALUATION

HISTOLOGIC ASSESSMENT OF NERVE FASCICLES. Treatment-related changes to periarterial nerves can be assessed using a semiquantitative ordinal grading system that allows the assessment of the type of

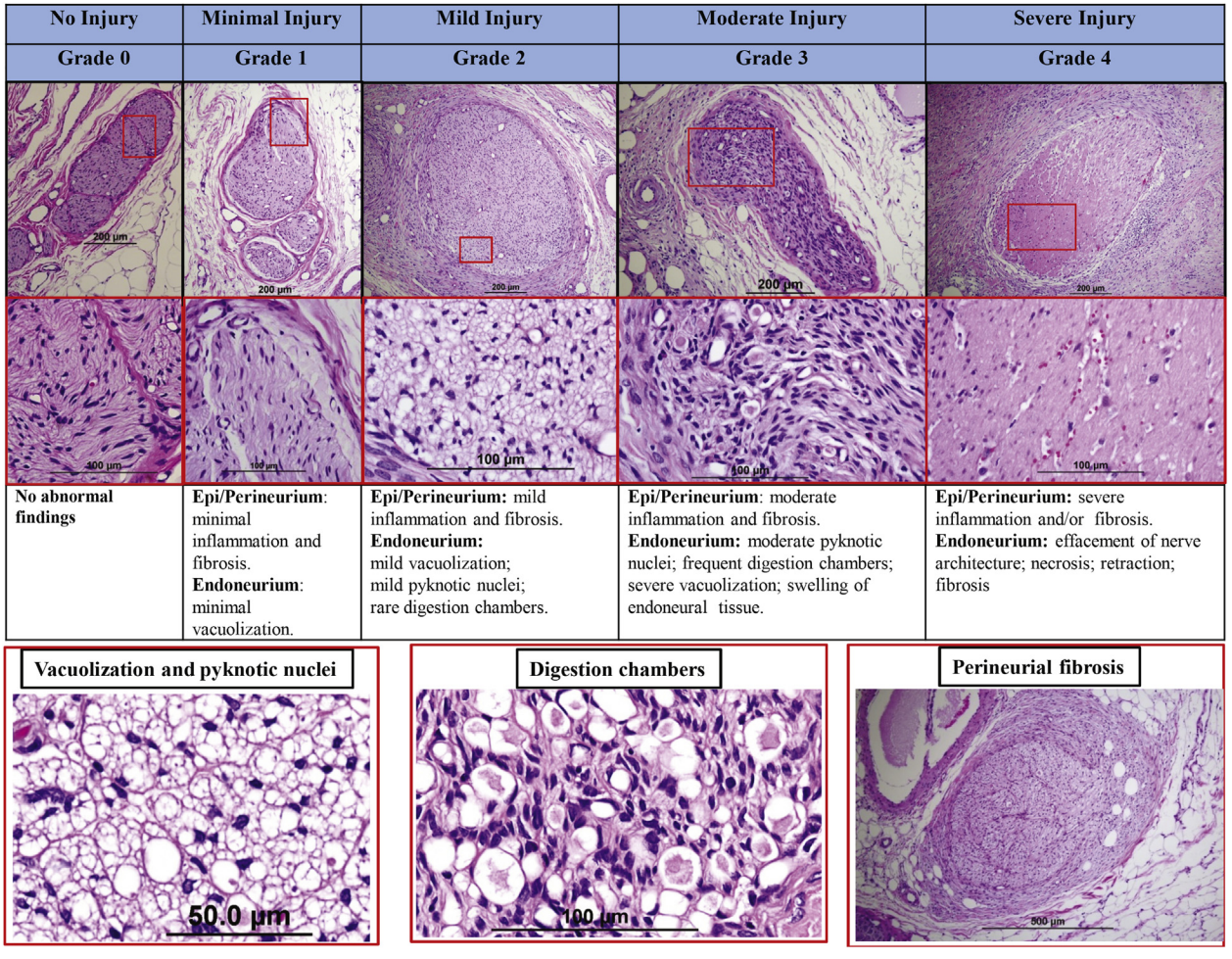

FIGURE 2 Semiquantitative Grading Scheme for Nerve Changes

(Upper) Representative images of nerves by increasing grade of injury. **(Middle)** High-power images of injured nerves **(red boxed area in upper panel)** in each grade. **(Lower)** Representative images of vacuolization, pyknotic nuclei, digestion chambers, and perineural fibrosis. Hematoxylin and eosin staining.

change (e.g., degeneration, necrosis, chronic) and its magnitude (e.g., minimal, mild, moderate, severe). Figure 2 provides a representative grading scheme that refers to effects on both peri- and endoneuronal tissue. The type and magnitude of changes in periarterial nerves can represent damage incurred directly with the treatment in the plane of section (i.e., nerves that lie directly in the path of treatment) or represent changes associated with injury to the nerve along its length outside the plane of section (i.e., upstream or downstream injury). Treatment may affect the perineuronal and/or endoneuronal portions of the renal nerves and present as degenerative, necrotic, or chronic changes. Degenerative changes associated with perineuronal or endoneuronal injury may include vacuolization and the formation of digestion chambers associated with injury, reversible or irreversible, to the axonal processes of the treated nerve. Necrotic changes may range from pyknosis/karyorrhexis of individual neural nuclei to coagulative necrosis or frank coagulation of the nerve bundle. After resolution of the acute phase of treatment, affected nerves may exhibit a variety of chronic changes including peri- and endoneural fibrosis, axonal atrophy, and loss. With minimal injury (i.e., grade 1), the nerve would be considered largely intact and likely functional, but exhibit subtle signs of damage that may include trivial perineuronal inflammation or hemorrhage and limited endoneuronal damage (perineuronal proteoglycan deposition, fibroplasia with little to no vacuolization, pyknosis, or increase in cellularity). With mild injury (i.e., grade 2), changes are more conspicuous and/or involve more of the nerve bundle and may include increased cellularity, perineuronal inflammation, fibrosis, and/or endoneuronal changes (e.g., vacuolization, pyknotic nuclei, digestion chambers). Nerves with moderate injury (i.e., grade 3) would be interpreted to exhibit more notable changes that may include perineuronal inflammation, fibrosis as well as endoneuronal damage (frequent pyknotic nuclei, digestion chambers, vacuolization, or swelling of endoneuronal tissue). Severe injury (i.e., grade 4) changes are typically overwhelming and may consist of marked perineuronal inflammation and/or fibrosis and endoneurium damage including effacement of nerve architecture, necrosis, and axonal retraction. Because minimal or mild injury (i.e., grade 2 or lower) can be seen even in untreated animals, moderate or severe injury (i.e., grade 3 or higher) should be considered a definite injury caused by thermal damage or toxins and generally correlates with decreases in renal norepinephrine levels.

Regardless of scoring methodology, the location of all observed nerves should be denoted relative to the area of the treatment (i.e., within or outside the zone of treatment) for the purposes of better understanding the treatment efficacy on the total population of nerves available for treatment.

IMMUNOSTAINING OF PERIVASCULAR NERVES AND SCORING CRITERIA

The intensity and distribution of immunostaining can be assessed using a semiquantitative scoring system (e.g., 0 = no reaction, 1 = patchy/very weak reaction, 2 = weak to moderate reaction, 3 = strong reaction). Representative images of immunostaining are shown in Figure 3. Typically, a weak reaction (i.e., grade 2 or lower) or the absence of TH represents a strong treatment effect as the absence of staining is an indirect sign of functional nerve degeneration and can be correlated with the renal norepinephrine levels. With respect to the functional assessment of nerve viability using immunostaining, the choice of time point is crucial as immunohistochemical analysis represents a snapshot assessment in the time course of axonal degeneration after RDN procedures. If the nerves being examined after <7 days of denervation, immunostaining is usually positive despite extensive necrosis; therefore, it is not recommended that immunostaining be performed before 7 days after the denervation procedure.

HISTOLOGICAL ASSESSMENT OF RENOVASCULAR MORPHOLOGY

Renovascular damage includes endothelial cell loss, thrombus formation, and medial damage, which can be assessed along the depth and circumference of the artery. These changes can be assessed using a semiquantitative ordinal grading system (e.g., 0 = none, 1 = minimal, 2 = mild, 3 = moderate, 4 = severe). Figure 4 provides representative images of a grading scheme that refers to both endothelial cell loss and medial wall damage. Endothelial cell loss should be evaluated by the percentage of circumferential endothelial cell loss (Figure 4). Endothelial cell loss is typically observed acutely after treatment and is rarely observed at 28 days. A common characteristic of thermal medial injury is smooth muscle cell loss/necrosis with proteoglycan and/or fibrous tissue replacement. The depth of medial damage is evaluated by the percentage of smooth muscle cell loss in relation to medial thickness (Figure 4). When evaluating the depth of medial damage, the presence of medial thinning should be reported. Medial thinning is

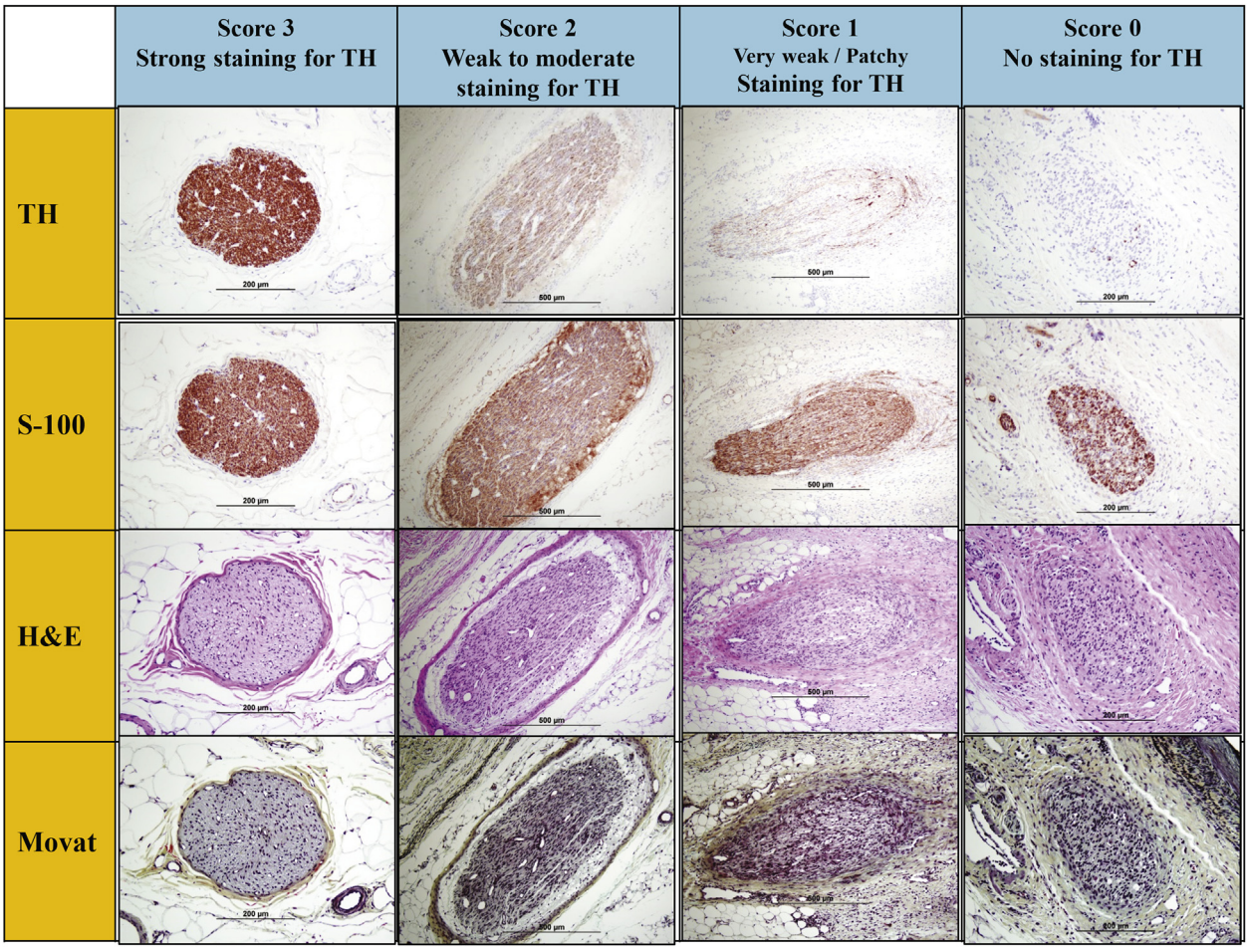

FIGURE 3 **Semiquantitative Scoring Criteria for Immunostain Against Tyrosine Hydroxylase**

(First Row) Representative images of injured nerves stained by anti-tyrosine hydroxylase (TH) enzyme. **(Second Row)** Corresponding images of injured nerves with S-100. **(Third Row)** Corresponding images of injured nerves with hematoxylin and eosin (H&E) stain. **(Fourth Row)** Corresponding images of injured nerves with Movat pentachrome stain.

defined as thickness of the media at the site of damage (in millimeters)/unaffected media thickness (in millimeters) with <0.5 representing severe smooth muscle cell loss/necrosis within the media. In addition, the cross-sectional dimension of medial damage can be assessed as circumferential loss/necrosis of smooth muscle cells. When evaluating medial damage, it is recommended to use the Movat pentachrome stain as proteoglycan deposition can be easily appreciated.

HISTOLOGICAL ASSESSMENT FOR PERIARTERIAL TISSUES AND ORGANS

Periarterial tissues such as fat, collagen, renal veins, arterioles, ureters, adrenal glands, skeletal muscle, viscera, and the kidneys should all be systematically evaluated for signs of injury. Again, a semiquantitative ordinal grading system (e.g., 0 = none, 1 = minimal, 2 = mild, 3 = moderate, 4 = severe) can be used to score observed changes. It is important to mention that the risk of thermal renal vein injury and thrombosis is far less than that of thermal arterial injury. Also, most venous injuries start at the abluminal surface, whereas most of arterial injuries begin at the luminal surface, depending, of course, on the mode of denervation used. However, as the veins are thin, it is important to appropriately assess the venous injury and/or thrombosis. Arteriolar damage usually correlates with the overall nerve damage. Typical severe (grade 4) injury of arterioles is fibrinoid necrosis, which is most often observed

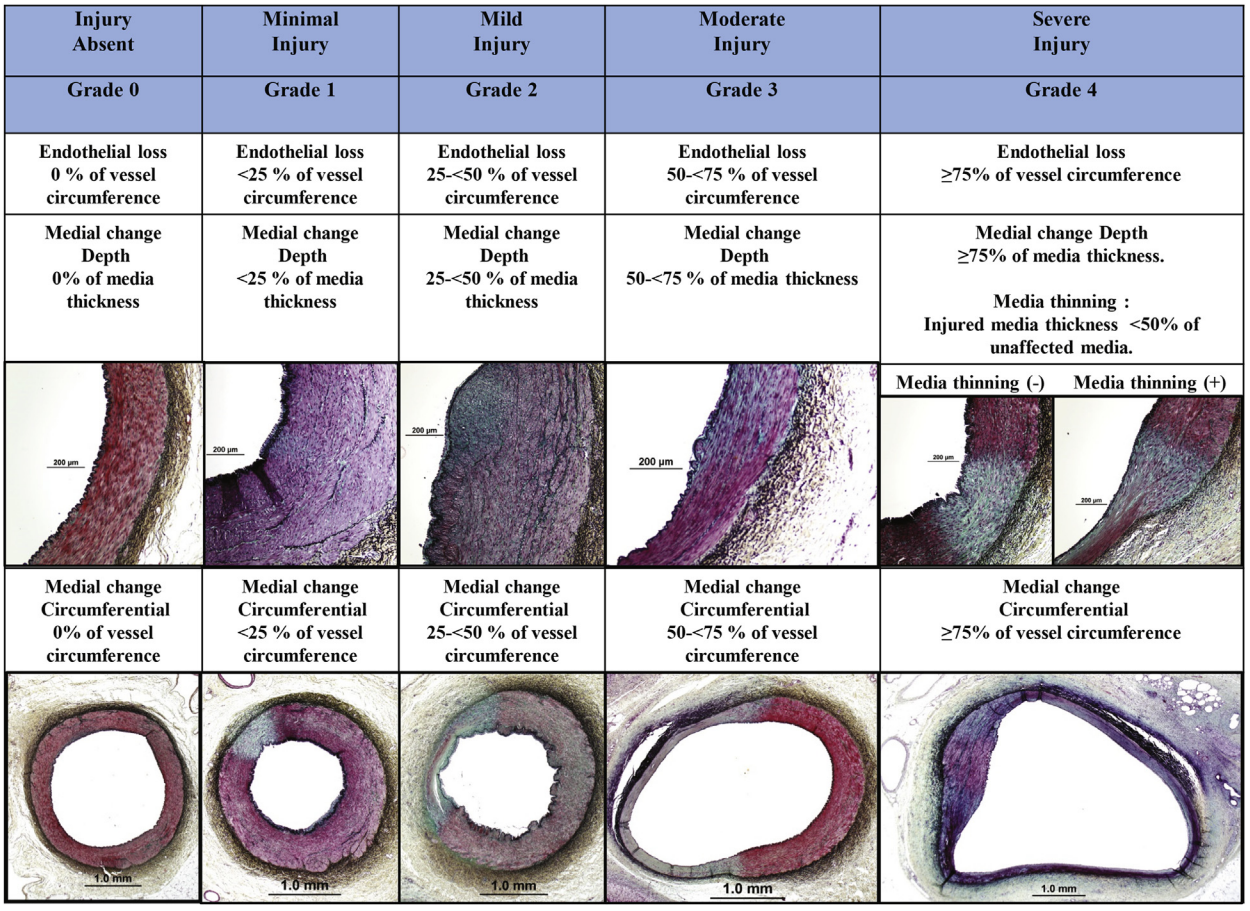

FIGURE 4 Semiquantitative Grading Scheme for Renal Artery Damage

(Upper) Images of the depth of medial wall injury by the grade of damage. **(Lower)** Represent circumferential grade of the damage of the medial wall. Note that medial thinning can only occur with grade 4 depth of injury and should be distinguished. All images are stained with Movat pentachrome.

acutely but often persists as long as 28 days. Representative scoring criteria for arteriole damage is shown in Online Figure 3. Injury to the ureters is evaluated by the extent of edema and necrosis (submucosal, muscular, and periureteral surrounding tissue) as well as mucosal ulceration. However, ureter injury is not frequent because the remote anatomic position of the ureter relative to the ablation site precludes it from direct thermal injury. As a direct sign of thermal injury of collagen/adipose tissue, the presence of denatured collagen should be assessed, which can easily be detected by elastica stains. Similarly, periadventitial fat may undergo necrosis with saponification and surrounding acute inflammation followed by chronic inflammation (25,26). This usually appears as a shadowy outline of adipose cells with saponification. Representative scoring criteria for fat damage are shown in Online Figure 4.

Not only are direct renal and soft tissue important, but attention should be also directed to lymph node damage, skeletal muscle, and adjoining viscera (e.g., the cecum and adrenal glands). Therefore, these structures should be routinely assessed by the individual necropsy prosector and submitted for histological assessment for the extent and type of damage, if present.

ADVANTAGE OF THE COMBINATION OF VARIOUS STAINS

The combination of an elastica stain with a standard H&E stain will more reliably allow the appropriate assessment of nerve injury, arterial wall injury, and

soft-tissue injury (Online Figure 5) as the information provided by both staining protocols is cumulative. For example, proteoglycan replacement (green tissue) within the arterial media can easily be recognized by a Movat pentachrome stain. Denatured collagen is clearly distinguished as black tissue by Movat pentachrome stain, whereas H&E gives a blue tinge of staining and may be difficult to identify. Also, perineural fibrosis can easily be recognized by Movat pentachrome stain. Therefore, we recommend using this stain as well as H&E routinely for the evaluation of arterial, soft-tissue, and nerve injuries.

QUADRANT ANALYSIS AND DEEPEST SOFT-TISSUE DAMAGE

To capture the entire spectrum of thermal and/or toxic tissue damage along the vascular circumference, a cross-sectional quadrant analysis is recommended, as shown in Online Figure 6, in which 1 quadrant refers to <25% circumferential area, 2 quadrants refer to 26% to 50% circumferential area, 3 quadrants refer to 51% to 75% circumferential area, and 4 quadrants refer to >75% circumferential area. Obtaining the number of quadrants with injured nerve fascicles relative to quadrants with the presence of nerve fascicles enables the capturing of differences in circumferential thermal injury among different devices. The distance from renal arterial lumen to the deepest tissue damage (nerves, vein, arterioles, or other soft tissues) determines the effective depth of thermal and/or toxic injury among different devices. **Figure 5** shows representative images of distance measurements. Combining the information retrieved from cross-sectional quadrant analysis and penetration of the depth of thermal injury provides unique information regarding the number of quadrants affected and the adequacy of the denervated area in relation to circumferential discontinuity of innervation of the kidney.

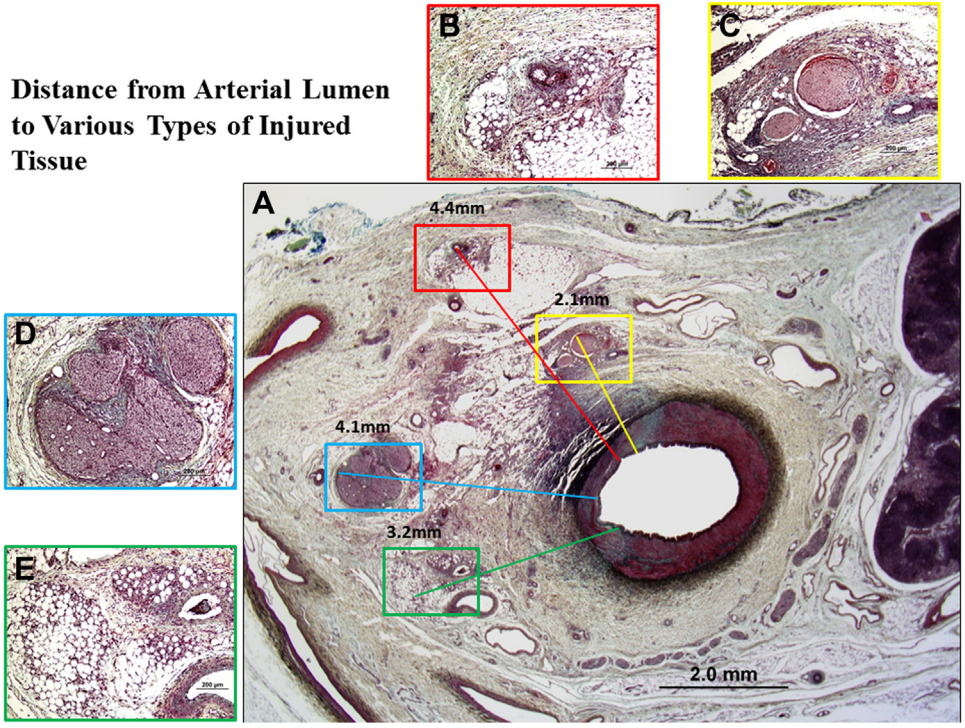

FIGURE 5 Representative Images of the Distance From the Arterial Lumen to Various Types of Injury

(A) Low-power image of a treated renal artery and surrounding perirenal area. **(B)** High-power images of injured arterioles **(red boxed area in A)**. The distance from the lumen to injured arterioles was 4.4 mm. **(C)** High-power image of nerve injury **(yellow boxed area in A)**. The distance from the lumen to injured nerves was 2.1 mm. **(D)** High-power image of injured nerves **(blue boxed area in A)**. The distance from the lumen to injured nerves was 4.1 mm. **(E)** High-power image of soft-tissue injury **(green boxed area in A)**. The distance from the lumen to injured tissue was 3.2 mm.

SUMMARY

A summary of methodological standard for the pre-clinical evaluation of RDN is shown in **Table 1**. The purpose of this paper is to guide and standardize the pre-clinical histopathological assessment with regard to renal sympathetic denervation procedures. Standardization of histopathological assessment remains an unmet need in this field, which may ultimately facilitate understanding of underlying mechanisms after RDN and further to help to assess which device is the more appropriate and what advantages each device may offer from the currently available technologies. As research in this area evolves, updates will be mandatory to warrant appropriate adoption into clinical practice.

REPRINT REQUESTS AND CORRESPONDENCE: Dr. Michael Joner, CVPath Institute, Inc., 19 Firstfield Road, Gaithersburg, Maryland 20878. E-mail: mjoner@cvpath.org.

TABLE 1 Summary of Methodological Standard for the Pre-Clinical Evaluation of Renal Sympathetic Denervation

Category	Methods	Purpose
Biomarker	Kidney norepinephrine levels (high-throughput tandem mass spectrometry)	Evaluation of the extent of renal sympathetic denervation
Macroscopic evaluation	TTC staining of renal artery	To assess the extent of arterial wall injury
Standard light microscopy and morphometry	Semiquantitative scoring of pathological changes (grade 0 to grade 4): nerve, renal artery, vein, arterioles, fat, and collagen	To determine the extent of nerve injury and arterial and surrounding soft-tissue injury
	Quadrant analysis (0 to 4 quadrants) for nerve injury and soft-tissue injury	Evaluation of circumferential extent of injury
	Depth of tissue injury, mm	Evaluation of therapeutic penetration
Immunohistochemistry	Semiquantitative scoring of intensity of immunostaining (score 0 to score 3) by anti-tyrosine hydroxylase	Evaluation of the ability of the nerves to generate norepinephrine (functional nerve injury)

TTC = 2,3,5-triphenyltetrazolium chloride.

REFERENCES

1. DiBona GF. Sympathetic nervous system and hypertension. Hypertension 2013;61:556–60.

2. Calhoun DA, Jones D, Textor S, et al. Resistant hypertension: diagnosis, evaluation, and treatment. A scientific statement from the American Heart Association Professional Education Committee of the Council for High Blood Pressure Research. Hypertension 2008;51:1403–19.

3. Esler MD, Krum H, Sobotka PA, Schlaich MP, Schmieder RE, Bohm M. Renal sympathetic denervation in patients with treatment-resistant hypertension (The Symplicity HTN-2 Trial): a randomised controlled trial. Lancet 2010;376:1903–9.

4. Rocha-Singh K. Renal artery denervation: a brave new frontier. Endovasc Today 2012; February:45–53.

5. Bhatt DL, Kandzari DE, O'Neill WW, et al. A controlled trial of renal denervation for resistant hypertension. N Engl J Med 2014;370:1393–401.

6. Berman LB. The Goldblatt kidney. Arch Intern Med 1971;128:306–8.

7. Katz MA, Shear L. Effects of renal nerves on renal hemodynamics. II. Renal denervation models. Nephron 1975;14:390–7.

8. Bello-Reuss E, Colindres RE, Pastoriza-Munoz E, Mueller RA, Gottschalk CW. Effects of acute unilateral renal denervation in the rat. J Clin Invest 1975;56:208–17.

9. Rippy MK, Zarins D, Barman NC, Wu A, Duncan KL, Zarins CK. Catheter-based renal sympathetic denervation: chronic preclinical evidence for renal artery safety. Clin Res Cardiol 2011;100:1095–101.

10. Tellez A, Rousselle S, Palmieri T, et al. Renal artery nerve distribution and density in the porcine model: biologic implications for the development of radiofrequency ablation therapies. Transl Res 2013;162:381–9.

11. Atherton DS, Deep NL, Mendelsohn FO. Micro-anatomy of the renal sympathetic nervous system: a human postmortem histologic study. Clin Anat 2012;25:628–33.

12. Krum H, Schlaich M, Whitbourn R, et al. Catheter-based renal sympathetic denervation for resistant hypertension: a multicentre safety and proof-of-principle cohort study. Lancet 2009;373:1275–81.

13. Esler M, Jennings G, Korner P, et al. Assessment of human sympathetic nervous system activity from measurements of norepinephrine turnover. Hypertension 1988;11:3–20.

14. Tsunoda M. Recent advances in methods for the analysis of catecholamines and their metabolites. Anal Bioanal Chem 2006;386:506–14.

15. Taylor RL, Singh RJ. Validation of liquid chromatography-tandem mass spectrometry method for analysis of urinary conjugated metanephrine and normetanephrine for screening of pheochromocytoma. Clin Chem 2002;48:533–9.

16. Ji C, Walton J, Su Y, Tella M. Simultaneous determination of plasma epinephrine and norepinephrine using an integrated strategy of a fully automated protein precipitation technique, reductive ethylation labeling and UPLC-MS/MS. Anal Chim Acta 2010;670:84–91.

17. Şenöz H. The chemistry of formazans and tetrazolium aalts. Hacettepe J Biol Chemy 2012; 40:293–301.

18. Bohl S, Medway DJ, Schulz-Menger J, Schneider JE, Neubauer S, Lygate CA. Refined approach for quantification of in vivo ischemia-reperfusion injury in the mouse heart. Am J Physiol Heart Circ Physiol 2009;297:H2054–8.

19. Bederson JB, Pitts LH, Germano SM, Nishimura MC, Davis RL, Bartkowski HM. Evaluation of 2,3,5-triphenyltetrazolium chloride as a stain for detection and quantification of experimental cerebral infarction in rats. Stroke 1986;17:1304–8.

20. Pace V, Perentes E, Germann PG. Pheochromocytomas and ganglioneuromas in the aging rats: morphological and immunohistochemical characterization. Toxicol Pathol 2002;30:492–500.

21. Burgi K, Cavalleri MT, Alves AS, Britto LR, Antunes VR, Michelini LC. Tyrosine hydroxylase immunoreactivity as indicator of sympathetic activity: simultaneous evaluation in different tissues of hypertensive rats. Am J Physiol Regul Integr Comp Physiol 2011;300:R264–71.

22. Harris T, Muller B, Cotton RG, Borri Voltattorni C, Bell C. Dopaminergic and noradrenergic sympathetic nerves of the dog have different L-DOPA decarboxylase activities. Neurosci Lett 1986;65:155–60.

23. DiBona GF, Esler M. Translational medicine: the antihypertensive effect of renal denervation. Am J Physiol Regul Integr Comp Physiol 2010;298:R245–53.

24. Liu L, Barajas L. The rat renal nerves during development. Anat Embryol (Berl) 1993;188:345–61.

25. Franco W, Kothare A, Ronan SJ, Grekin RC, McCalmont TH. Hyperthermic injury to adipocyte cells by selective heating of subcutaneous fat with a novel radiofrequency device: feasibility studies. Lasers Surg Med 2010;42:361–70.

26. Smith GW, Rotstein DS, Brownie CF. Abdominal fat necrosis in a pygmy goat associated with fescue toxicosis. J Vet Diagn Invest 2004;16:356–9.

KEY WORDS immunohistochemical stains, pathology, pre-clinical, renal denervation, renal norepinephrine concentration

APPENDIX For a supplemental methods section and figures, please see the online version of this article.